Acta Acustica united with Acustica
Vol. 101 (2015) 986 – 992

DOI 10.3813/AAA.918893

Tunable Broadband Acoustic Gain in Piezoelectric Semiconductors at ε-Near-Zero Response

Johan Christensen, Morten Willatzen
Department of Photonics Engineering, Technical University of Denmark, 2800 Kgs. Lyngby, Denmark.
willatzen@gmail.com

Summary
Piezoelectric semiconductors have emerged as materials capable to amplify sound waves when electrons are set to drift at supersonic speeds. Several experiments have demonstrated this behaviour at moderate amplification levels for some intrinsic semiconductors and carrier concentrations. On a theoretical basis we show that amplification of sound can be significantly enhanced when the materials are operated close to the plasma frequency. If the drifting carriers collectively oscillate with the plasma the electromechanical coupling is enhanced since the permittivity is related inversely proportional to the mechanical stress and vanishes near the bulk plasma frequency. By optically or electrically doping GaAs and InSb as exemplified in this work, we predict that amplification of sound can be achieved effectively for a bandwidth exceeding several decades making this active system very attractive for loss-compensation in metamaterials and applicable for sensing such as nonlinear devices. The paper contains a detailed derivation and discussion of transmission and reflection coefficients for pressure pulses impinging on a semiconductor slab and the acoustic gain enhancement that can be achieved by dynamic switching of the electric field as well as tuning flexibility through dynamic control of the carrier density.

PACS no. 43.35.+d, 42.79.Dj, 81.05.Xj

1. Introduction

Recent developments in structured materials and acoustic metamaterials have hitherto exclusively relied on passive building blocks. These passive building block consisting of metallic or fluid scatterers are commonly constructed to form a crystal with enriched wave properties as compared to what nature can offer by conventional materials. When speaking about acoustic material properties we focus on dynamical processes rather than relying on static characteristics. This means that the dispersive nature of crystals very much dictates the desired way an acoustic wave would respond. Thus, relying on diffraction effects or resonances we have witnessed the creation of unusual wave propagation behaviours in the form of negative refraction [1, 2, 3], acoustic cloaks of invisibility [4, 5] and unusal strong absorptions [6, 7, 8, 9] to name a few. These passive structures gain their effects by geometrical means such that for example the dispersion relation or effective parameters can be tuned by controlling the size and shape of individual elements (meta-atoms).

Real-life applications demand active control of devices without the need of physically altering or modifying the structure. There are numerous passive applications such as acoustic rectifiers or barriers in the form of phononic crystals or metamaterials that would benefit substantially by active control [10, 11]. By external electrical or optical stimuli coupled to, for example, magneto-rheological fluids or piezoelectric materials that are capable to hybridize with acoustic functionalities as named above, one could spectrally tune the formation of forbidden bands of sound propagation or actively control uni-directional radiation. Active acoustic devices have successfully been realized by the aid of electronic components. In one example linear non-reciprocity has been designed in an acoustic circulator where electric fans create resonance mode splitting such that sound can propagate along selective paths only [12]. A different active design is based on a nonlinear device consisting of a sub-wavelength helmholtz resonator that can be electronically switched to permit sound propagation in one direction but not in the opposite one [13].

Instead of imposing active control to structured metamaterials and surfaces by means of a coupling medium or likewise, we investigate here electronic control of various piezoelectric semiconductors and their capabilities to act as active materials.

When an external acoustic field irradiates a piezoelectric semiconductor slab as depicted in Figure 1, a coherently oscillating electric charge is created. Superimposing a sufficiently high dc electric field corresponding to a supersonic carrier drift speed leads to sound amplification

Received 24 February 2015,
accepted 26 May 2015.

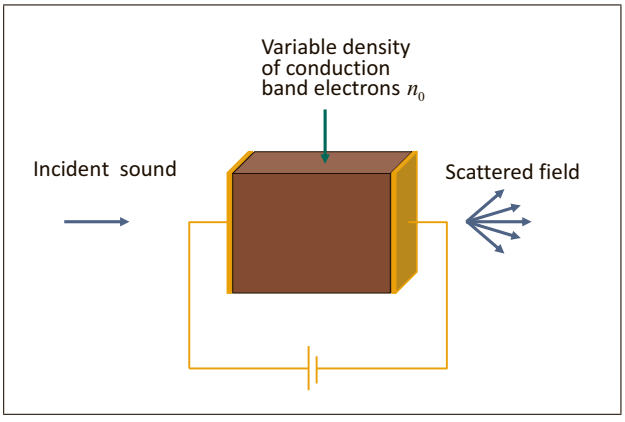

Figure 1. Sketch of the active piezoelectric semiconductor analyzed within this work. Sound waves are incident from left to right and emerges the structure at the slab far-side. An external dc voltage is applied to ensure that the electric field E_0 inside the material sets the charge into supersonic motion. Additional we sketch the possibility of externally varying the density of conduction band electrons n_0, which, e.g., can be realized by photo-excitation or electrostatic gating.

by virtue of phonon emission; an effect known as acoustic Cherenkov radiation [15]. Amplification of sound has been first observed by Hutson et al., followed by numerous other theoretical and experimental investigations confirming this striking finding [14, 16, 17]. We have recently reported a giant increase in the amplification of sound in the THz range if InSb is operated in the close proximity to the bulk plasma frequency, i.e., for ε-near-zero (ENZ) conditions [18]. This intriguing behavior has not only led to advanced phase control and super-squeezing of waves [19, 20, 21, 22] but also to the possibility of creating electric levitation [23]. Figure 1 illustrates an externally applied dc field that is needed to set charges into supersonic motion, but beyond that, it can also be used to actively increase the amount of gain produced [18]. By modifying the electron density n_0 one can alter the plasma frequency ω_p of the bulk semiconductor over a spectrally rich domain. In doing so it can be foreseen that acoustic gain assisted by the ENZ response may lead to an additional degree of freedom where the bandwidth can be controlled externally.

In this work we present a thorough study on the realization of acoustic gain associated with ENZ conditions close to the plasma frequency. We conduct numerical simulations to demonstrate this behavior in the MHz and THz range, respectively, for two piezoelectric semiconductor materials, GaAs and InSb, and furthermore illustrate how the spectral response can be broadened to several decades for a specific semiconductor material if the carrier concentration is modified. A detailed discussion of gain in transmission and reflection, including derivation of transmission and reflection coefficients, is also presented for an electrically controlled semiconductor slab. Further we show how gain can be further enhanced by switching the sign of the applied field leading to amplification of sound in both forward and backward direction inside a slab. In a practical realization there are several techniques available to modify the plasma frequency ω_p of a semiconductor. Introducing dopants to the intrinsic semiconductor obviously is one way. But without modifying the bulk of the structure one could also apply a variable electrostatic gating or externally control the carrier concentration by photo-excitation of the material. These multidisciplinary approaches are readily available to conduct full active control of the amplification of sound aiming at various important applications. Metamaterials, whose counterintuitive properties rely on collectively oscillating elements, inevitably display large ohmic losses. Optical metamaterials based on metallic structures suffer from high dissipative losses and diminish the intended revolutionary effect of negative refraction. To counteract this, active gain materials (e.g., laser dyes) have been incorporated in these structures in order to effectively compensate losses [24, 25]. Many recent experiments on acoustic metamaterials similar to the optical case exhibit loss restrictions induced by resonances and friction. As we will see in the following, owing to the spectrally rich response of acoustic gain which actively is tuned via external stimuli, we envision that piezoelectric semiconductors could be incorporated into acoustic metamaterial systems.

2. Theoretical framework

We begin the analysis by considering the constitutive relations for a piezoelectric material,

$$\mathcal{T} = cS - eE, \tag{1}$$

$$D = \varepsilon E + P + eS, \tag{2}$$

where $\mathcal{T}$, S, D, E, P, c, e, and ε are the stress, strain, electric displacement, electric field, spontaneous polarization, stiffness, piezoelectric e constant, and the permittivity, respectively. The equations above are usually represented by tensor equations, however, by regarding field variations along the coordinate x only, treating the physics as a scalar problem is sufficient for the present analysis. In the constitutive relations Eq. (1) and Eq. (2) we apply the Onsager relationship, losses on the other hand, will be accounted for by using a finite and frequency-dependent complex carrier mobility. We will use a Drude model for the real part of the permittivity in Equation (2),

$$\varepsilon = \varepsilon_\infty \varepsilon_0 \left(1 - \frac{\omega_p^2}{\omega^2 + \tau^{-2}}\right), \tag{3}$$

where ε_∞ is the high-frequency relative permittivity, ε_0 is the vacuum permittivity, ω is the angular frequency, τ is the average collision time between carriers, and ω_p is the plasma frequency,

$$\omega_p = \sqrt{\frac{nq^2}{\varepsilon_\infty \varepsilon_0 m_{eff}}}. \tag{4}$$

Here n is the density of conduction band electrons, q is the positive electron charge, and m_{eff} is the electron effective

mass. The complex mobility μ_n is written as

$$\mu_n = \mu_{low}\frac{\tau^{-1}}{\tau^{-1}+\mathrm{i}\omega}, \tag{5}$$

where μ_{low} is the dc mobility, and the conductivity follows from

$$\sigma_n = qn\mu_n. \tag{6}$$

As we mentioned earlier, we begin by considering electromechanical wave motion only along x. For this we apply Newton's second law on the stress and Equation (1) to obtain the resulting wave equation

$$\rho\frac{\partial^2 u}{\partial t^2} = \frac{\partial \mathcal{T}}{\partial x} = c\frac{\partial^2 u}{\partial x^2} - e\frac{\partial E}{\partial x}, \tag{7}$$

where ρ is the mass density and $S = \frac{\partial u}{\partial x}$ with u the material displacement. Next, we are going to regard the electronic part of the problem. In the first place, we consider only electrons and discard the presence of holes. The continuity equation reads

$$\frac{\partial J}{\partial x} = -\frac{\partial \rho_e}{\partial t}, \tag{8}$$

where J and ρ_e are the free current density and the space charge density, respectively. Let n_s be the carrier density due to the presence of an acoustic field. The total density n of electrons in the conduction band is given by

$$n = n_0 + f n_s, \tag{9}$$

where f denotes the fraction of the acoustically generated carriers that are free to move (not bound to, e.g., states in the energy gap) and n_0 is the carrier density in equilibrium. Since the background ion charge exactly compensates for the carrier density in equilibrium, the free charge satisfies

$$\rho_e = -qn_s, \tag{10}$$

where q is the magnitude of the electron charge. The free current density J due to electrons comprise both contributions from drift and diffusion and is written as

$$J = q\mu_n nE + qfD_n\frac{\partial n_s}{\partial x}, \tag{11}$$

where μ_n and D_n are the electron mobility and electron diffusion constant, respectively and n_0 is constant in space, $\partial n_0/\partial x = 0$. They are connected by the Einstein equation

$$D_n = \frac{\mu_n k_b T}{q}, \tag{12}$$

where k_b and T are the Boltzmann constant and the temperature (in Kelvin), respectively. Finally, we need the Maxwell-Poisson equation

$$\frac{\partial D}{\partial x} = \rho_e = -qn_s. \tag{13}$$

If we differentiate the latter expression with time and combine Equations (8)–(11) we arrive at

$$\frac{\partial^2 D}{\partial x \partial t} = f\mu_n E\frac{\partial^2 D}{\partial x^2} - qn_0\mu_n\frac{\partial E}{\partial x} + f\mu_n\frac{\partial D}{\partial x}\frac{\partial E}{\partial x} + fD_n\frac{\partial^3 D}{\partial x^3}. \tag{14}$$

In deriving the above expressions it has been assumed that holes are too heavy to move in the presence of an electric field (similar assumption is done for the ions and possible dopants). In this case, space charges can solely exist due to the presence and movement of conduction electrons. This assumption is in accordance with the fact that for most semiconductors the hole mobility and hole diffusion constants are much smaller than their electron counterparts. Further, the hole effective mass is much larger than the electron effective mass. Hence, the charge and current contributions from holes are insignificant.In order to solve Equation (14) we seek harmonic solutions. Consider therefore the case where the electric field is a sum of dc and AC components,

$$E = E_0 + E_1\exp\left(\mathrm{i}\omega t - \mathrm{i}kx\right). \tag{15}$$

If the AC component is small enough we may neglect products of terms involving AC components (small-signal analysis). We also write

$$D = D_0 + D_1\exp\left(\mathrm{i}\omega t - \mathrm{i}kx\right), \tag{16}$$

$$u = u_0(x) + u_1\exp\left(\mathrm{i}\omega t - \mathrm{i}kx\right), \tag{17}$$

where E_0, D_0 are constants and $u_0(x)$ is a time-independent function of x. Using this Ansatz, we find from Equation (14)

$$D_1 = \frac{iqn_0\mu_n k}{\omega k + f\mu_n E_0 k^2 - \mathrm{i}fD_n k^3}E_1 \equiv \gamma E_1. \tag{18}$$

Further, from the constitutive relation Equation (2), we then have

$$E_1 = -\mathrm{i}\frac{ke}{\frac{\mathrm{i}qn_0\mu_n k}{\omega k + f\mu_n E_0 k^2 - \mathrm{i}fD_n k^3} - \varepsilon}u_1 \equiv \delta u_1. \tag{19}$$

Using the latter expression in Equation (8), the following dispersion equation is found:

$$\rho\omega^2 = ck^2 - \frac{k^2 e^2}{\frac{\mathrm{i}qn_0\mu_n}{\omega + f\mu_n E_0 k - \mathrm{i}fD_n k^2} - \varepsilon}. \tag{20}$$

This expression can be recast as a fourth-order polynomial equation,

$$\alpha_4 k^4 + \alpha_3 k^3 + \alpha_2 k^2 + \alpha_1 k + \alpha_0 = 0, \tag{21}$$

$$\begin{aligned}
\alpha_0 &= -\frac{\rho\omega^2}{c}\left(1 - \mathrm{i}\frac{\sigma_0}{\varepsilon\omega}\right),\\
\alpha_1 &= -f\mu_n\rho E_0\frac{\omega}{c},\\
\alpha_2 &= 1 + \frac{e^2}{\varepsilon c} + \mathrm{i}fD_n\frac{\rho}{c}\omega - \mathrm{i}\frac{\sigma_0}{\varepsilon\omega},\\
\alpha_3 &= \frac{f\mu_n E_0}{\omega}\left(1 + \frac{e^2}{\varepsilon c}\right),\\
\alpha_4 &= -\frac{\mathrm{i}fD_n}{\omega}\left(1 + \frac{e^2}{\varepsilon c}\right),
\end{aligned} \tag{22}$$

where $\sigma_0 = qn_0\mu_n$. It is possible to simplify Equations (21) and (22) substantially if we neglect small terms of second order or higher order in the mobility μ_n leading effectively to a second order polynomial equation in k (refer to the section below). This simplification is in accordance with the fact that $|k'| \gg |k''|$ expressing the complex roots as $k = k' + \mathrm{i}k''$.

3. Dynamic transmission and reflection

In this section we present analytical derivations for the transmission coefficient of sound through a slab of a piezoelectric semiconductor controlled by an external dc electric field and/or varying the carrier density. The piezoelectric semiconductor slab thickness is L and the carrier density in the absence of acoustic excitation is n_0. The two wavenumber solutions k_1 and k_2 are

$$\begin{aligned}
k_1 &= \sqrt{\frac{\rho}{c - \frac{e^2}{\beta_1 - \epsilon}}}\omega,\\
k_2 &= -\sqrt{\frac{\rho}{c - \frac{e^2}{\beta_2 - \epsilon}}}\omega,\\
\beta_1 &= \frac{\mathrm{i}\sigma}{\omega + f\mu_n E_0 k_0 - \mathrm{i}fD_n k_0^2},\\
\beta_2 &= \frac{\mathrm{i}\sigma}{\omega - f\mu_n E_0 k_0 - \mathrm{i}fD_n k_0^2},
\end{aligned} \tag{23}$$

where

$$k_0 = \sqrt{\frac{\rho}{c + \frac{e^2}{\epsilon}}}\omega. \tag{24}$$

These expressions apply to first order in the mobility μ_n, i.e., k_0 is a solution to Eqs. (21) and (22) when $\mu_n = 0$ such that $\alpha_1 = \alpha_3 = \alpha_4 = 0$ [note that by virtue of Equation (12) it also follows that $D_n = 0$ when $\mu_n = 0$]. For frequencies in the MHz-THz range, we have $\beta_1 \approx \beta_2$ and thus $k_1 \approx -k_2 \equiv k$ since the imaginary part of the wavenumbers k_1, k_2 is many orders of magnitude smaller than the corresponding real part. Therefore, the travel times in passing through the slab in forward and backward directions are the same and the acoustic speed in the semiconductor is

$$v = \sqrt{\frac{c - \frac{e^2}{\beta_1 - \epsilon}}{\rho}}. \tag{25}$$

The structure consists of three layers where the acoustic impedance of the semi-infinite medium to the left of the slab is Z_1, the piezoelectric slab impedance is $Z \equiv Z_2 = \rho v$, and the acoustic impedance of the semi-infinite medium to the right of the slab is Z_3. We will now consider an incoming (from the left) acoustic signal consisting of pulses with repetition period $2L/v >> \frac{2\pi}{\omega}$ and $Z_0 \equiv Z_1 = Z_3$. This repetition period ensures that the part of the first pulse that is transmitted into the piezoelectric medium and makes a single roundtrip in the slab returns to the left slab boundary exactly when the second pulse arrives at the slab, and so forth as we outlined in [18].

If the incoming pulse pressure on the slab is one ($p_{in} = 1$), the pressure just after reflection of the first pulse at the left slab boundary is r_{12} at time $t_R(1) = 0$ where

$$r_{lm} = \frac{Z_m - Z_l}{Z_m + Z_l}. \tag{26}$$

Similarly, the transmission coefficient of the first pulse into layer 3 is $t_{12}\exp(-\mathrm{i}kL)t_{23}$ at time $t_T(1) = L/v$ where

$$t_{lm} = 1 + r_{lm}. \tag{27}$$

Since the acoustic signal consists of pulses repeated in time as mentioned above, we find the following reflection coefficient at the left slab boundary,

$$\begin{aligned}
R\left[t_R(j+1)\right] = R\left[t_R(j)\right] &+ t_{12}\exp\left(-\mathrm{i}kL\right)r_{23}\\
&\cdot \exp\left(\mathrm{i}kL\right)t_{21}\\
&\cdot \left(r_{21}\exp\left(-\mathrm{i}kL\right)r_{23}\exp\left(\mathrm{i}kL\right)\right)^{j-1},
\end{aligned} \tag{28}$$

at times

$$t_R(j+1) = j\frac{2L}{v}, \tag{29}$$

where j is 1,2,3,... For the transmission coefficient we have

$$\begin{aligned}
T\left[t_T(j+1)\right] = T\left[t_T(j)\right] &+ t_{12}\exp\left(-\mathrm{i}kL\right)r_{23}\\
&\cdot \exp\left(\mathrm{i}kL\right)r_{21}\exp\left(-\mathrm{i}kL\right)t_{23}\\
&\cdot \left(r_{21}\exp\left(-\mathrm{i}kL\right)r_{23}\exp\left(\mathrm{i}kL\right)\right)^{j-1},
\end{aligned} \tag{30}$$

where

$$t_T(j+1) = t_T(1) + j\frac{2L}{v}, \tag{31}$$

and j is 1,2,3,... The above analysis can be carried out in a similar way in the case where the dc electric field sign is switched at times $L/v, 2L/v, 3L/v, \ldots$. In this way the ultrasonic pulse experiences gain in traversing the piezoelectric slab in both directions and the pressure contributions add together for the incoming train of pulses specified by

the signal repetition rate. The expressions for R and T then become

$$\begin{aligned} R\left[t_R(j+1)\right] &= R\left[t_R(j)\right] + t_{12}\exp\left(-\mathrm{i}k_1L\right)r_{23} \\ &\quad\cdot\exp\left(\mathrm{i}k_2L\right)t_{21} \\ &\quad\cdot\left(r_{21}\exp\left(-\mathrm{i}k_1L\right)r_{23}\exp\left(\mathrm{i}k_2L\right)\right)^{j-1}, \\ T\left[t_T(j+1)\right] &= T\left[t_T(j)\right] + t_{12}\exp\left(-\mathrm{i}k_1L\right)r_{23} \\ &\quad\cdot\exp\left(\mathrm{i}k_2L\right)r_{21}\exp\left(-\mathrm{i}k_1L\right)t_{23} \\ &\quad\cdot\left(r_{21}\exp\left(-\mathrm{i}k_1L\right)r_{23}\exp\left(\mathrm{i}k_2L\right)\right)^{j-1}. \end{aligned} \tag{32}$$

3.1. Tuning of plasma frequency

The carrier density and thus the plasma frequency in a semiconductor slab can be controlled by application of electric fields and light [26]. Illumination of light is an effective way to uniformly generate carriers, over many orders of magnitude, in a semiconductor slab that decay at a rate determined by the carrier lifetime. Thus, generation occurs at a fast rate governed by the dynamics of the light field. Recombination of electron-hole pairs, is expected to be the limiting factor for switching and occurs by virtue of through traps/impurities (proportional to n), light emission (proportional to n^2), or by Auger processes (proportional to n^3; in this case with a small carrier density Auger recombination is not important) in the semiconductor e.g. due to the addition of dopants. In this way (adding dopants), the recombination rate can be increased significantly to allow for fast switching. Thus, it is possible to modify the recombination rate substantially [10^{-8} – 10^{-12} sec] for GaAs by adding, e.g., Si or Ge dopants. The application of large electric fields, e.g. in the direction perpendicular to the direction of sound propagation, is another possible way to increase the carrier density through impact ionization. The details of these studies, theoretically and experimentally, are very relevant but outside the scope of the present work.

4. Numerical results and dicussions

From the previously derived analytical dispersion relation, it can be easily shown that when $\epsilon = 0$ the imaginary part of k can take on arbitrarily large positive or negative values and occurs whenever $\omega^2 = \omega_p^2 - \tau^{-2}$. Hence, only where the plasma frequency is larger than the inverse carrier collision time $\omega_p\tau > 1$ as is the case for, e.g., intrinsic InSb and GaAs, amplification of sound can be pronounced due to strong electromechanical coupling associated with the plasma oscillation. For these two named materials and some specific material parameters we will put this to the test.

In Figure 2 we plot the complex wavenumbers k_1 and k_2 for GaAs by computing the above given dispersion relation Equation (21) while discarding higher-order contributions. In the caption of Figure 2 we indicate the various material parameters leading to a low plasma frequency $f = 15.7$ MHz. The imaginary part Im(k), characterizing the strength of acoustic gain or absorption, and the sign of

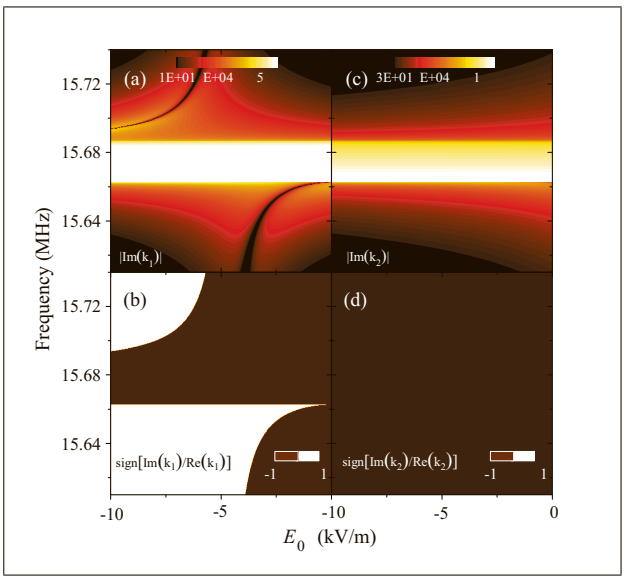

Figure 2. (Color online) Electromechanical response at ENZ conditions with frequencies around the plasma frequency for GaAs. We have used the following parameters: $e = -0.16$ C/m^2, $c = 8.55 \cdot 10^{10}$ Pa, $m_{eff} = 0.063$ (in units of the free-electron mass), $\rho = 5320$ kg/m^3, $n_0 = 2.1 \cdot 10^{12}$ m^{-3}, $\mu_{low} = 0.85$ m^2/s/V, $\epsilon_\infty = 10.89$, $\tau = m_{eff}\mu_{low}/q$, and $F = 1$ corresponding to a plasma frequency $f = 15.7$ MHz. The two wavenumbers k_1 and k_2 are calculated as a function of electric field and frequency in the MHz regime. (a) |Im(k_1)|, and (b) illustrating the sign of the ratio of the real and imaginary parts of k_1. (c) and (d) as in the latter case, now plotting for k_2. Colorbar units are in m^{-1}.

the fraction Im(k)/Re(k) are plotted versus the externally applied electric field E_0 and the frequency. Both roots k_1 and k_2, as seen in Figure 2a and Figure 2c, are characterized by large imaginary parts close to the plasma frequency where the permittivity goes to zero resulting in strong electromechanical coupling. Note that a positive (negative) sign of the ratio Im(k)/Re(k) corresponds to acoustic gain (attenuation). This is illustrated in Figure 2b and Figure 2d showing that acoustic amplification only sustains for the k_1 wavenumber since there the sign can be positive. Contrary to this it is seen that k_2 acoustic wave propagation always is characterized by a negative sign of the ratio Im(k)/Re(k) hence no gain is supported by k_2 acoustic waves. As we mentioned earlier, the imaginary part of k can have extremely large values meaning that sound amplification may lead to large large amplitudes when operating at ENZ conditions. What is important to consider but not an aspect within this paper is the possible saturation of gain as a result of nonlinear sound interaction and increased material absorption.

With the same parameters as simulated in Figure 2, we fix the external field at $E_0 = -8.0$ kV/m to ensure supersonic drift but vary the charge concentration n_0 over several decades spanning from 2×10^{12} upto 2×10^{20}m^{-3} as illustrated in Figure 3. The plasma frequency as expressed by Equation (4) strongly depends on the concentration of charge carriers n_0. Piezoelectric semiconductors therefore provide promising tunable materials when, e.g.,

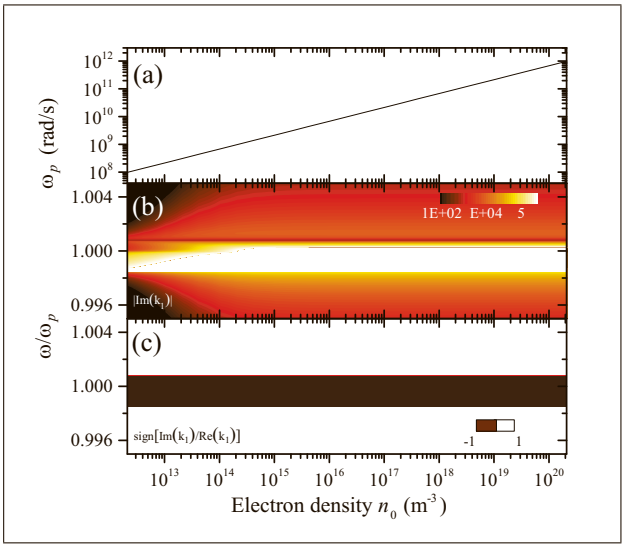

Figure 3. (Color online) Via a variation in the electron density n_0 the plasma frequency of GaAs can be tuned over a broad spectral window spanning several decades, see (a). (b) $|\mathrm{Im}(k_1)|$, and (c) illustrating the sign of the ratio of the real and imaginary parts of k_1. We have chosen not to plot k_2 in here. Colorbar units are in m^{-1} and $E_0 = -8.0\ kV/m$.

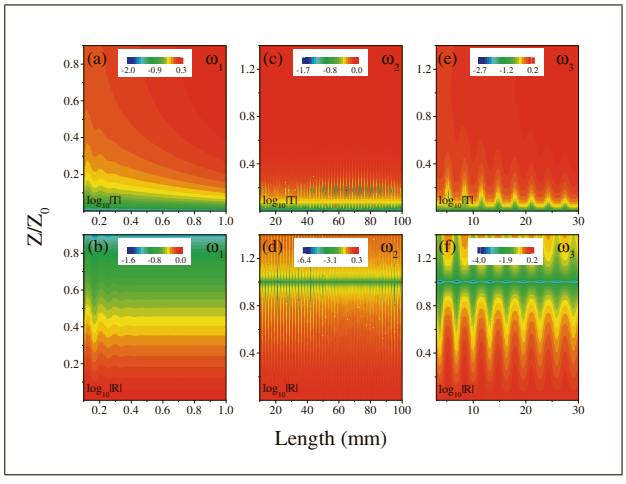

Figure 4. (Color online) Simulated transmission coefficient T and reflection coefficient R for three different frequencies plotted against the impedance mismatch Z/Z_0 and the slab length L. For InSb we have $\omega_p = 1.7 \cdot 10^{13}$rad/s and $\omega_1 = 0.995\omega_p$, $\omega_2 = 0.95\omega_p$, $\omega_3 = 0.997\omega_p$. In this simulation an external stationary electric field is applied.

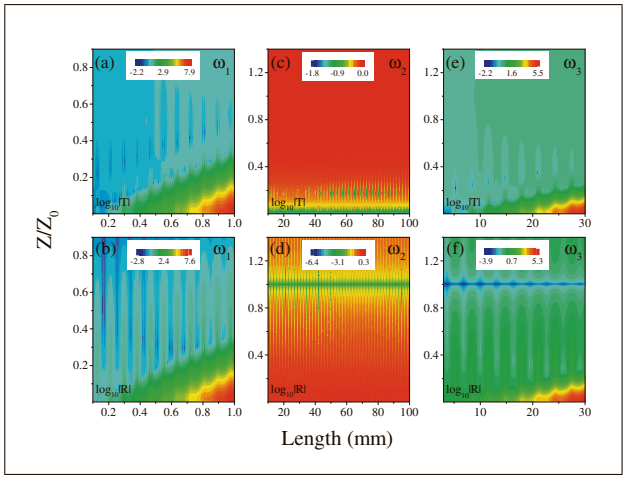

Figure 5. (Color online) Same as in the previous figure except that dynamical switching of the dc field at a frequency equal to $L \cdot \mathrm{Re}(k)/\omega$ is invoked.

electrically charged, such that ENZ conditions can be controlled in a representative frequency window in the range from MHz to THz as illustrated in Figure 3a. By plotting the contour of $\mathrm{Im}(k_1)$ in Figure 3b we predict that strong acoustic gain can be sustained over several frequency decades (but always for a spectral region in close proximity to the plasma frequency) where the permittivity takes values near zero and $\mathrm{Im}(k)/\mathrm{Re}(k) > 0$ as seen in Figure 3c. These simulations show that sound amplification can be actively controlled by choosing the semiconductor material, the level of doping, and by electrostatic gating or photoexcitation. Thus, one can determine the proper spectral response and utilize this technique for interesting metamaterials-related applications such as active loss-compensation.

Next, we consider a few applications associated with the possibility of producing acoustic gain in piezoelectric semiconductor materials. For this, we consider sound traversing a finite slab made of, e.g., InSb and apply the theory as developed in the previous section. We calculate the transmission and reflection coefficients for various values of the impedance mismatch Z/Z_0 and the slab length as illustrated in Figure 4. We choose as well three representative frequencies that are in near proximity of the plasma frequency. The frequencies ω_1 and ω_3 are selected such that the permittivity is very close to zero. In all panels we predict oscillations with the length stemming from standing wave resonances within the slab. The upper panels in Fig. 4, representing the transmission coefficient in a log scale, show that the cases with frequencies ω_1 and ω_3 lead to amplification since the transmission coefficient is larger than unity. Albeit not easy to see in the plots, our calculations further reveal the intuitive result that when the slab is poorly matched to its surrounding, i. e., $Z << Z_0$, reflection dominates over transmission.

In order to further amplify the present gain values we suggest a method, as already discussed in the theory part, by periodically switching the sign of the applied field in time with a period equal to $L \cdot \mathrm{Re}(k)/\omega$. Introducing switching of this type will amplify the sound field both in forward and backward direction inside the slab since the sign of the damping term $\mathrm{Im}(k)$ is controlled by the sign of the applied field $E_0(t)$ [18].

Hence, for the system discussed in the former example, we now introduce switching and observe that for the cases with frequencies slightly below ω_p gain is further enhanced as seen in the panels of Figure 5 representing transmission and reflection coefficients for ω_1 and ω_3, respectively. Since ω_2 is the farthest from the ENZ condition, switching has only minimal influence on the radiated

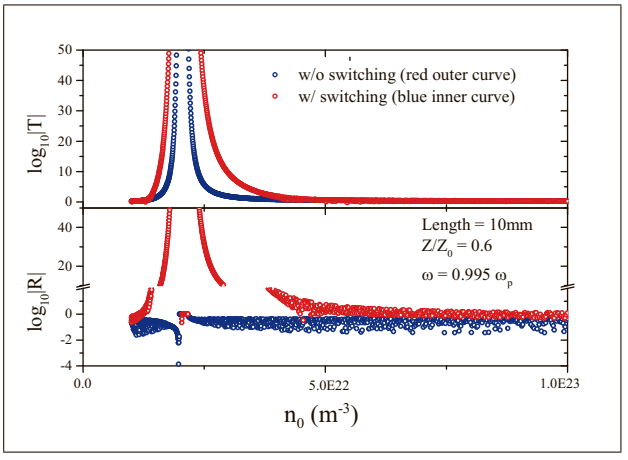

Figure 6. (Color online) An InSb slab is irradiated by sound and we plot the transmission (T) and reflection (R) coefficients as a function of equilibrium density n_0 for a fixed frequency. Two scenarios are simulated for the two cases without and with switching invoked. Other parameters are given in the legends.

sound field. Finally, as discussed in connection with Figure 3 where it was demonstrated how spectral tuning can be accomplished via variations in the charge density, we will discuss how sound scattering is also influenced by n_0. We lock the frequency to ω_1 and take the slab thickness to be 10mm. Surrounding the InSb slab such that $Z = 0.6Z_0$ we compute the transmission and reflection coefficients for some specific values of the charge density n_0 as depicted in Figure 6. It can be clearly observed that there is an optimal charge density value giving rise to a pronounced peak in T and R. In other words, sound propagation through a piezoelectric semiconductor slab is not only amplified through the length effect but varying n_0 as well as modulating E_0 at every acoustic round trip provide full control in generating enhanced acoustic gain for many interesting applications.

5. Conclusion

We have shown that piezoelectric semiconductors like GaAs and InSb give rise to strong electromechanical coupling when assisted by collective plasma oscillations where the permittivity is near zero - ENZ. Apart from the regimes where acoustic waves are always attenuated we demonstrated that sound waves are significantly amplified when operated at ENZ conditions. These properties benefit from the electrical tunability of semiconductors which in the present case allows to actively control and modulate the plasma frequency associated with strong gain. We have presented a detailed derivation and discussion of transmission and reflection coefficients for pressure pulses impinging on a semiconductor slab and the benefit in acoustic gain that can be achieved by dynamic switching of the electric field.

We foresee that acoustic gain operated at the ENZ response will stimulate future experimental work. Although sound amplification has been experimentally observed already in the sixties by Hutson et al [14], the giant enhancement by the plasma oscillation and active control of carrier concentration and electric field to ensure strong gain over several decades bandwidth could open new avenues in the possibility to tailor the flow of sound. Acoustic metamaterials have been engineered to work at several frequencies beyond the audible range. Miniaturing devices for future applications will automatically scale the operating frequencies up to the MHz regime and above. Furthermore, dealing with these resonating structures one will unfortunately always be accompanied by ohmic losses. For this reason, we believe that active loss-compensation by piezoelectric semiconductors could be readily available.

Acknowledgments

J. C. gratefully acknowledges financial support from the Danish Council for Independent Research and a Sapere Aude grant (12-134776).

References

[1] Z. Liang et al., Sci. Rep. **3**, 1614 (2013).
[2] Y. Xie, B.-I. Popa, L. Zigoneanu and S. A. Cummer, Phys. Rev. Lett. **110**, 175501 (2013).
[3] V. M. Garcia Chacano, J. Christensen and J. Sanchez-Dehesa, Phys. Rev. Lett. **112**, 144301 (2014).
[4] N. Stenger, M. Wilhelm and M. Wegener, Phys. Rev. Lett. **108**, 014301 (2012).
[5] L. Sanchis, et al., Phys. Rev. Lett. **110**, 124301 (2013).
[6] J. Mei et al., Nat. Comm. **3**, 756 (2012).
[7] J.Z. Song, P. Bai, Z. H. Hand and Y. Lai, New J. Phys. **16**, 033026 (2014).
[8] P. Wei et al., Appl. Phys. Lett. **104**, 121902 (2014).
[9] J. Christensen *et al.*, Sci. Rep. **4**, 4674 (2014).
[10] M. Kadic et al., Rep. Prog. Phys. **76**, 126501 (2013).
[11] M. Maldovan, Nature **503**, 209 (2013).
[12] R. Fleury et al., Science **343**, 516 (2014).
[13] B. Popa and S. A. Cummer, Nat. Comm. **5**, 3398 (2014).
[14] A. R. Hutson, J. H. McFee and D. L. White, Phys. Rev. Lett **7**, 237 (1961).
[15] D. L. White, J. Appl. Phys. **33**, 2547 (1962).
[16] A. R. Hutson and D. L. White, J. Appl. Phys. **33**, 40 (1962).
[17] V. I. Pustovoit, Sov. Phys. Usp. **12**, 105 (1969).
[18] M. Willatzen and J. Christensen, Phys. Rev. B **89**, 041201 (R) (2014).
[19] B. Edwards, A. Alu, M. E. Young, M. Silveirinha, and N. Engheta, Phys. Rev. Lett. **100**, 033903 (2008).
[20] R. Maas, J. Parsons, N. Engheta and A. Polman, Nat. Photonics **7**, 907 (2013).
[21] N. Engheta, Science **340**, 286 (2013).
[22] R. Fleury and A. Alu, Phys. Rev. Lett. **111**, 055501 (2013).
[23] F. J. Rodriguez-Fortuno et al., Phys. Rev. Lett. **112**, 033902 (2014).
[24] S. Xiao et al., Nature **466**, 735 (2010).
[25] S. Wuestner et al., Phys. Rev. Lett. **105**, 127401 (2010).
[26] L. Wang, W. Cai, X. Zhang, J. Xu, arXiv:1406.4274v1 [cond-mat.mes-hall] 17 Jun (2014).